# On the identification of $Sb_2Se_3$ using Raman scattering

A. Shongalova[1,2], M. R. Correia[1], B. Vermang[3,4,5], J. M.V. Cunha[6], P. M.P. Salomé[6,7#] and P. A. Fernandes[1,6,8]

(1) Departamento de Física and I3N, Universidade de Aveiro, 3810-193 Aveiro, Portugal

(2) Satpayev University, Satpayev street, 22a, 050013 Almaty City, Kazakhstan

(3)University of Hasselt – partner in Solliance, Agoralaan gebouw H, Diepenbeek, 3590, Belgium

(4)Imec – partner in Solliance, Kapeldreef 75, Leuven, 3001, Belgium

(5)Imomec – partner in Solliance, Wetenschapspark 1, Diepenbeek, 3590, Belgium

(6) International Iberian Nanotechnology Laboratory ,4715-330 Braga,Portugal

(7)Departamento de Física, Universidade de Aveiro, 3810-193 Aveiro, Portugal

(8) CIETI, Departamento de Física, Instituto Superior de Engenharia do Porto, Instituto Politécnico do Porto, Rua Dr. António Bernardino de Almeida, 431, 4200-072 Porto, Portugal

# corresponding author: P.M.P. Salomé - pedro.salome@inl.int

**Abstract***:* Robust evidences are presented that show that the Raman mode close to 250 cm$^{-1}$ in $Sb_2Se_3$ thin films does not belong to this binary compound. A study of the Raman spectrum power dependency revealed the formation of $Sb_2O_3$ for high values of power excitation when these measurements are done in normal atmospheric conditions. In order to complement this study, $Sb_2Se_3$ thin films were annealed to mimic the thermal conditions of Raman measurements and characterized by X-ray diffraction technique. These measurements showed that the compound $Sb_2Se_3$ can be replaced by $Sb_2O_3$ under those conditions and a heat-assisted chemical process explains these findings. Furthermore, it is shown what the Raman conditions that are needed for correct measurements to be performed.

**Introduction**

The semiconductor compound $Sb_2Se_3$ has recently shown to have many interesting properties for several applications: thermoelectric[1], energy storage devices[2–4], solar cells[1,5–9], among others. $Sb_2Se_3$ can be prepared in polycrystalline thin films with the orthorhombic crystalline structure using standard (both atmospheric pressure or vacuum based) thin film growth techniques like electrodeposition[10] or thermal evaporation[5,11], just to name a few. $Sb_2Se_3$ appears to be in the same class of materials as the chalcogenides $Cu(In,Ga)Se_2$ (CIGS), CdTe, $Cu_2ZnSn(S,Se)_4$ (CZTSSe), i.e. they have excellent optoelectronic properties and are self-doped semiconductors. Their doping is intrinsic to their crystalline structure and depends heavily on their growth parameters and properties. Hence, the correct identification of the $Sb_2Se_3$ crystalline structure and the correct use of the corresponding identification techniques, are of the utmost importance for the advancement of this material as an application on optoelectronic devices.

For a proper identification of the $Sb_2Se_3$ structural phase, and also of the correct stoichiometry[12,13], researchers have turned their attention to Raman scattering (RS). RS is widely used

for the identification of main and secondary phases of chalcogenide materials as it is a non-destructive technique and allows for very fast interpretations. Moreover, in the chalcogenide materials, RS usually allows for the identification of the dominant phases without superimposition problems, as it can occur in x-ray diffraction[14]. With regards to $Sb_2Se_3$, in the literature, the peaks at 190 $cm^{-1}$ and 250 $cm^{-1}$ are usually attributed to Sb-Se and Sb-Sb bonds, respectively[11,15,16]. However, the peak around 250 $cm^{-1}$, has many interpretations and conflicting origins[15,17,18]. In fact, part of the assignment's problem arises from the fact of several selenium phases and antimony oxides having peaks close to that region as shown in Table I. As the correct identification of which phases and structures will allow for a better understanding of the $Sb_2Se_3$ growth mechanisms and properties, in this work we will show that: i) the 250 $cm^{-1}$ peak does not belong to the $Sb_2Se_3$ phase and ii) RS measurements done at high laser power conditions lead to oxidation of the sample surface.

**Experimental procedure**

The $Sb_2Se_3$ thin films were grown according to a method described in detail elsewhere[19] and were prepared by a two-step process. Se-rich Sb-Se thin films were sputtered from a $Sb_2Se_3$ sputtering target (Stanford Advanced Materials) with a 99.99% purity, followed by a rapid thermal annealing at 300 °C with $H_2Se$ during 15 minutes. Composition was analyzed using Energy Dispersive Spectroscopy and the composition ratio, [Se]/[Sb], is 1.9, which by comparing with the stoichiometric value of 1.5, implies that the overall sample is Se rich. Such fact is normal in this kind of samples as widely reported, due to condensation of Se during the cooling down of the film. Optical reflectance measurements allowed the estimation of a direct absorption close to 1.0 eV. Details of these studies are presented elsewhere[19]. The RS measurements were done in the backscattering configuration using a 632 laser line with a 50 X long range distance lens. Cooling and heating was achieved by using a cold-finger substrate under $N_2$ from -196 °C to 600 °C (THMS600 Linkam microscope stage). The crystalline phase identification was complemented with X-ray diffraction measurements and the results indicate that orthorhombic *Pbnm* (62) $Sb_2Se_3$ is the dominant phase.

*Table I - Main RS peaks of several phases that may originate during the growth of Sb2Se3. As explained further in the text, the orthorhombic Sb2Se3 is intentionally without a peak at 250 cm-1 and this region is highlighted in the other phases.*

| Compound | Structure | Raman shift ($cm^{-1}$) | Supporting references |
|---|---|---|---|
| $Sb_2Se_3$ | orthorhombic | 80,120,151, 189, 210 | this work, [20] |
| $Sb_2O_3$ | cubic | 82, 189, 254, 373,450 | [18], this work |
| $Sb_2O_4$ | | 72, 142, 199, 255, 400, 463 | [18] |
| $Se_n$ (spiral chains) | trigonal | 141, 234, 237 | [14,17,21], this work |
| $Se_8$ (rings) | α-monoclinic | 112, 253 | [17,21] |
| $Se_6$ (rings) | rhombohedral | 67-72, 102, 129, 221, 247 | [17] |
| Red Se (rings) | amorphous | 250 | [14,17,21] |

| Sb | rhombohedral | 110, 150 | [22] |
|---|---|---|---|

## Results and discussion

In Figure 1 we present the Raman spectra of a $Sb_2Se_3$ film, measured for different power values of the incident laser line, ranging from 70 µW to ~790 µW. The Raman spectra show a pronounced dependence on the excitation. We note that similar studies carried out on orthorhombic $Bi_2S_3$ nanostructures[23] also have shown a strong dependence on power excitation. In our case, all of the Raman spectra display peaks at 153 $cm^{-1}$, 189 $cm^{-1}$ and 210 $cm^{-1}$ commonly assigned to the $Sb_2Se_3$ phase. Under low power conditions there is a double peak at 234 $cm^{-1}$ and 238 $cm^{-1}$ which we attribute to trigonal Se[17], the most stable phase of Selenium[21]. The presence of such peak is consistent with the EDS measurements that showed a slight Se-rich film composition, and consequently, Se can condensate at the sample´s surface[24,25], which is very common in the preparation of this kind of samples.  Intriguing is the evolution of the spectrum with increasing excitation power. It should be noted that for the lowest laser power, no peak at ~ 250 $cm^{-1}$ is observed, in spite of this being one of the peaks commonly reported in the Raman studies of $Sb_2Se_3$[11,15,16,26]. As the  laser power increases, together with the appearance of the ~ 250 $cm^{-1}$ peak other peaks ( ~ 80 $cm^{-1}$, ~ 372 $cm^{-1}$, and ~ 450 $cm^{-1}$ ) are detected whose intensities follow the increase on the intensity of the ~ 250 $cm^{-1}$ peak,  suggesting that they are likely connected.  Furthermore, Figure 1 shows a clear decrease of the double peak located at ~ 235 $cm^{-1}$ with increasing RS laser power until it vanishes, for the highest power value. On the other hand, the peak located at 190 $cm^{-1}$ remains, within the experimental error, stable in position and integrated intensity but its FWHM decreases by about 2 $cm^{-1}$. The well-known laser heating effect always causes anharmonic effects in solids, evidenced by a broadening and a red shift of the Raman bands[27], and simultaneously, under high power or prolonged laser irradiation, structural transitions and crystalline changes may occur due to long-range ordering, as well as local or macroscopic ordering[28]. At first glance one might think that the decrease of the FWHM of the peak at 190 $cm^{-1}$ is related to the local annealing of the $Sb_2Se_3$ phase, which results in an improvement in the crystalline quality of the material. However, if this would be the case, one would expect a gradual increase in intensity throughout the experiment, which is not observed. Consequently, it is unlikely that the peaks at 190 $cm^{-1}$ and 250 $cm^{-1}$ could be correlated, thus, we do not attribute the 250 $cm^{-1}$ peak to the $Sb_2Se_3$ orthorhombic phase. The appearance of the 250 $cm^{-1}$ peak will be discussed further in the text.

By comparing the values at ~ 80 $cm^{-1}$, ~189 $cm^{-1}$, ~ 372 $cm^{-1}$ and ~ 250 $cm^{-1}$ and  ~ 450 $cm^{-1}$ for the several phases summarized in Table I, these peaks correspond to a $Sb_2O_3$ phase. Previous Raman studies do not mention the power used and such experiments are commonly performed in air atmosphere. Those evidences lead us to affirm that the commonly reported Raman spectra are measured under high laser power conditions since the presence of the Raman peak at ~250 $cm^{-1}$ is only observed in our measurements with high excitation power conditions.  In addition, due to the excess of Se in the films, Se phases are also a candidate to explain the existence of a Raman band at ~250 $cm^{-1}$, that is related with the vibration mode of $Se_8$ and $Se_6$ rings[17]. Taking into account the EDS results, showing an inhomogeneous Se distribution, different points of the sample were probed by Raman. Figure 2 relates to a cross section measurement, in air, close to the glass substrate, i.e. as further away from the surface of the film as possible. We do not expect Se condensation and oxidization of a fresh cleavage cross-section. Although the signal-to-noise ratio worsens, no peak at 250 $cm^{-1}$ is observed by increasing the laser power, and the

observed main peaks can only be assigned to the $Se_2Se_3$ phase. These results indicate that in this region the film has a well-defined stoichiometry, avoiding the probability of oxidation of Sb or the contribution of selenium condensates.
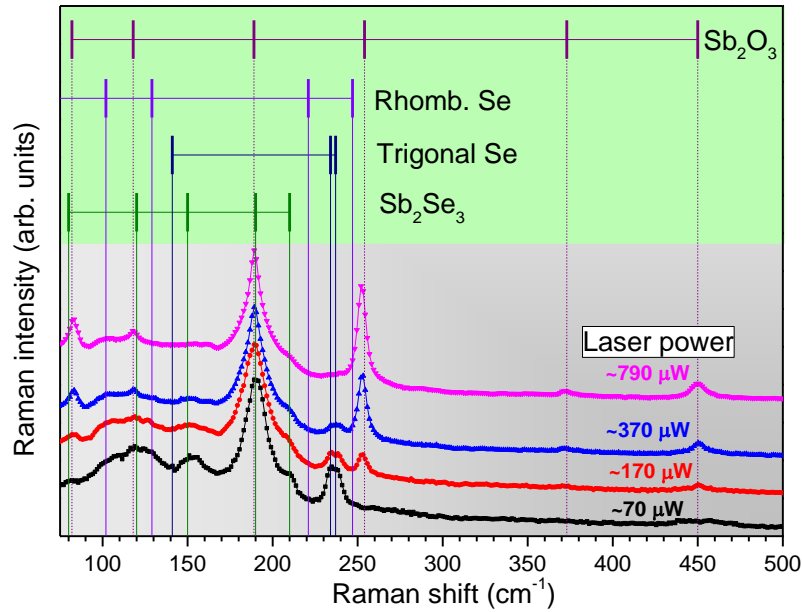


Figure 1: Study of Raman spectrum dependence on the excitation laser power for a $Sb_2Se_3$ film at room temperature. Under the lowest laser power the peak at 250 cm$^{-1}$ is absent in spite of several $Sb_2Se_3$ peaks being present.
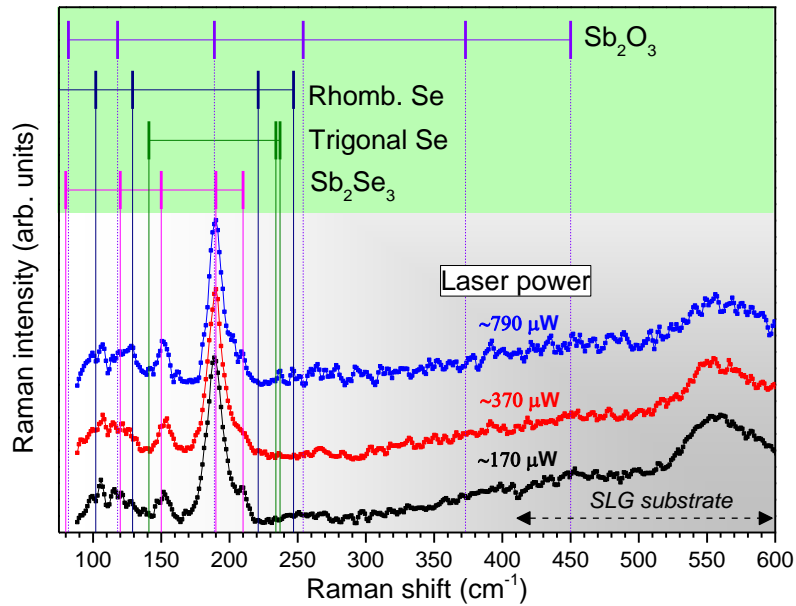


Figure 2: Raman spectrum dependence on the excitation laser power measured for the cross section of the analyzed film, in a spot close to the glass substrate.

All the Raman peaks observed in Figure 1 and Figure 2 are within the expected range of frequencies when compared with the Raman frequencies reported for the lighter $Sb_2S_3$ isostructural phase[29]. The group theory predicted for the $Sb_2Se_3$ unit cell of five non-equivalent sites, thirty zone-center Raman actives phonon modes belonging to the irreducible representation:

5

$\Gamma_{Raman} = 10\,A_g + 10\,B_{1g} + 5\,B_{2g} + 5\,B_{3g}$. Removing the zero-frequency acoustic phonon modes, a total of twenty seven optical Raman modes are expected[29,30]. In spite of the huge number of phonons expected, only few peaks have been observed in the Raman studies reported so far[15,16,20,31,32]. In the Raman study reported by Y. Zhao et al[23] for high quality samples of $Bi_2S_3$ material, which is also isostructural to $Sb_2Se_3$, the number of experimental Raman peaks observed is higher than the commonly observed ones for $Sb_2Se_3$. In that work, the comparison between theoretical and experimental frequencies was possible considering an adjustment process involving the entire Raman spectrum, neglecting other contributions. We note that if $Sb_2Se_3$ and $Bi_2S_3$ are isostructural with the orthorhombic crystalline phase, then, one would expect the peaks of both phases to be visible close in energy positions and with the same number of modes. Such fact is true if we discard the 250 cm$^{-1}$ peak. Such occurrence is another indication to the hypothesis that this peak is not from the $Sb_2Se_3$ phase. As the crystalline structure of $Sb_2O_3$ is cubic, its Raman peaks should be significantly different in energy position and number of nodes compared with $Sb_2Se_3$, which is the case for the peak around 250 cm$^{-1}$.

With the quality of the films investigated here, we cannot neglect other effects that may contribute to the observed Raman spectrum. In order to understand the RS peaks positions of $Sb_2Se_3$, we started to study the stability of the phase as function of incident RS laser power. In other chalcopyrite materials, like for instance CIGS and CZTS, one needs to use relatively low values of laser intensity in order to avoid damage to the film itself. The damage usually comes in 3 forms: i) structural changes that induced different symmetry space groups[28]; ii) evaporation of atoms of some elements which leads to a change in the structure[27]; and iii) incorporation and/or replacement of elements from the atmosphere, namely oxygen[27]. All of these changes have the potential to be thermodynamically available by the energy delivered by the laser exposure. In this particular case, the amount of energy available to catalyze the possible changes comes from the laser intensity and from relative long exposure times.

Having demonstrated further evidence that the $Sb_2Se_3$ phase should not have the 250 cm$^{-1}$ peak, we will now explore its appearance. As previously referred, the appearance of new peaks, while changing the laser intensity, can be a consequence of several causes. Since the FWHM values and the peak positions of the $Sb_2Se_3$ phase are kept the same as function of laser power, we can discard structural changes since these would change the lattice parameters and/or change the space group leading to significant changes in the RS peaks. If the 250 cm$^{-1}$ peak is to be associated with a $Sb_2O_3$ phase, then, oxygen can only come from two sources: i) oxygen already present on the sample surface due to air exposure after growth and/or b) oxygen present in the air.

To test the oxygen origin hypothesis, we performed a Raman laser power dependency in low-vacuum conditions. In this case, we are not capable of having high resolution due to the vacuum window and the samples are likely locally heated to higher temperature values due to lack of convection and thus some peak position energy shifts might occur. Figure 3 shows the results, at low power the same results as in the previous test are found: i) the $Sb_2Se_3$ can be identified with peaks at 153 cm$^{-1}$, 189 cm$^{-1}$ and 210 cm$^{-1}$; ii) the trigonal Se phase is present with a double peak at 234 cm$^{-1}$ and 239 cm$^{-1}$. With increasing laser power, we see the same trend as observed previously: the double peak corresponding to trigonal Se lowers significantly while the $Sb_2Se_3$ peaks suffer very minor changes. At the highest laser power values, a small peak around 250 cm$^{-1}$ is present and no traces of the peak at 372 cm$^{-1}$ are to be found. These results tend to indicate that under vacuum, the Se excess at the sample surface is removed, however, due to the lack of oxygen from the air, the formation of $Sb_2O_3$ is vastly reduced. The oxygen source can be attributed

both to small amounts of oxygen adsorbed at the sample surface and to remaining oxygen still present in the low-vacuum conditions of the measurement.
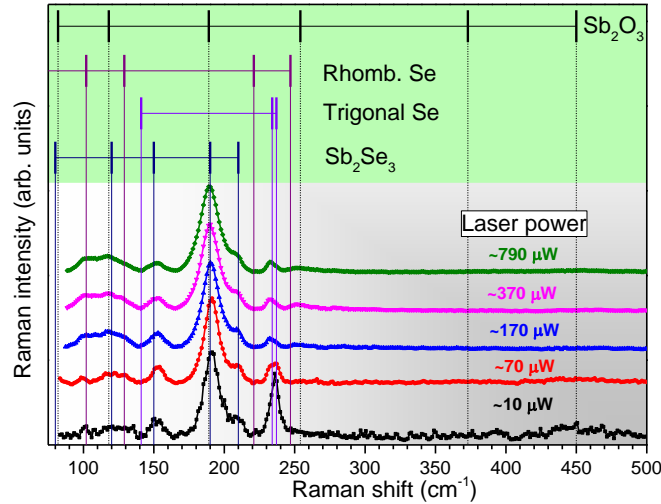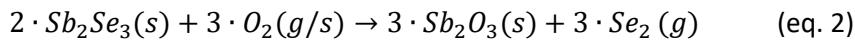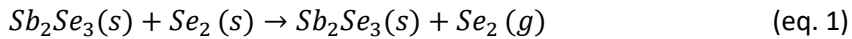


*Figure 3: Raman laser power dependency test in low-vacuum conditions. With increasing power it is observable a lowering of the peak associated with selenium and only a very small and broad peak at 250 cm$^{-1}$ is found at high power conditions. The peaks attributed to the phase Sb$_2$Se$_3$, 153 cm$^{-1}$, 189 cm$^{-1}$ and 210 cm$^{-1}$, remain unchanged.*

The findings of the previous experiments allow us to conclude that, contrary to the literature, the peaks at 250 cm$^{-1}$ and 372 cm$^{-1}$ do not belong to Sb$_2$Se$_3$, but belong rather to Sb$_2$O$_3$. Furthermore, we hypothesize that the formation of the Sb$_2$O$_3$ is due to Se replacement by oxygen and resulting Se is simply evaporated due to its high vapor-pressure. The two-step reaction is represented by eq.1 and eq2:

$$Sb_2Se_3(s) + Se_2(s) \rightarrow Sb_2Se_3(s) + Se_2(g) \qquad \text{(eq. 1)}$$

$$2 \cdot Sb_2Se_3(s) + 3 \cdot O_2(g/s) \rightarrow 3 \cdot Sb_2O_3(s) + 3 \cdot Se_2(g) \qquad \text{(eq. 2)}$$

This system has not been studied in detail and no trusty values of enthalpy energies are available to evaluate the reactions likelihood. These reactions fit the observed results and thermodynamic studies are needed to validate them.

In order to validate even further our results, we present evidence of the energy-induced oxidation of the sample by a temperature-dependence XRD study shown in Fig. 4. At low temperature conditions, the XRD is dominated by the Sb$_2$Se$_3$ orthorhombic peaks[33]. The temperature was increased in air atmosphere, performing effectively an air-annealing. At the temperature of 450 °C, the spectrum starts to be dominated almost exclusively by the Sb$_2$O$_3$ diffraction peaks[33]. This result is further evidence that with enough energy, Sb$_2$Se$_3$ decomposes into Sb$_2$O$_3$. As with the Raman analysis, due to the significant difference in the crystalline structure between Sb$_2$Se$_3$ and Sb$_2$O$_3$, the diffraction pattern is significantly different as well.

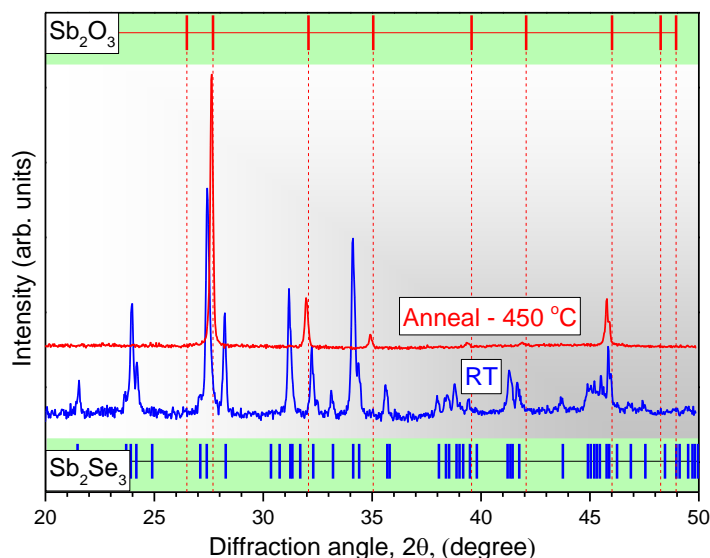*Figure 4: Diffractogram of a Sb2Se3 thin film at room temperature and after an annealing in air at a temperature of 450 $o^C$33.*

## Conclusions

In this work, we showed that the identification of $Sb_2Se_3$ using Raman scattering must be performed in low power conditions, ~100 µW, in order to avoid the Se evaporation and the oxidation of the $Sb_2Se_3$ phase. The prominent peak around 250 $cm^{-1}$ which is usually attributed to $Sb_2Se_3$ in the literature, belongs in fact to $Sb_2O_3$. The origin of the $Sb_2O_3$ is due to oxidation. In order to avoid oxidation during RS measurements and to perform more reliable measurements, at high laser excitation power conditions it is recommended to perform this technique in vacuum or in an inert atmosphere environment. Alternatively, Raman Scattering measurements of $Sb_2Se_3$ should be done at very low power conditions. We note that the observation of oxidation is true for a variety of measurements that are done in air and that provide some energy to the samples like XRD, photoluminescence, photoconductivity, etc. An important observation of our work is also related with the stability of the $Sb_2Se_3$ compound: high energy conditions, like excitation laser power or temperature, easily lead to the formation of a $Sb_2O_3$ phase, thus, synthesis processes have to account for this fact when preparing the compound.

## Acknowledgements

## REFERENCES

[1] H.C. Kim, T.S. Oh, and D.-B. Hyun, J. Phys. Chem. Solids **61**, 743 (2000).

[2] M.-Z. Xue and Z.-W. Fu, J. Alloys Compd. **458**, 351 (2008).

[3] J. Ma, Y. Wang, Y. Wang, Q. Chen, J. Lian, and W. Zheng, J. Phys. Chem. C **113**, 13588 (2009).

[4] W. Luo, A. Calas, C. Tang, F. Li, L. Zhou, and L. Mai, ACS Appl. Mater. Interfaces **8**, 35219 (2016).

[5] L. Wang, D.-B. Li, K. Li, C. Chen, H.-X. Deng, L. Gao, Y. Zhao, F. Jiang, L. Li, F. Huang, Y. He, H. Song, G. Niu, and J. Tang, Nat. Energy **2**, 17046 (2017).

[6] Y. Zhou, L. Wang, S. Chen, S. Qin, X. Liu, J. Chen, D.-J. Xue, M. Luo, Y. Cao, Y. Cheng, E.H. Sargent, and J. Tang, Nat. Photonics **9**, 409 (2015).

[7] C. Chen, Y. Zhao, S. Lu, K. Li, Y. Li, B. Yang, W. Chen, L. Wang, D. Li, H. Deng, F. Yi, and J. Tang, Adv. Energy Mater. **7**, 1700866 (2017).

[8] C. Chen, L. Wang, L. Gao, D. Nam, D. Li, K. Li, Y. Zhao, C. Ge, H. Cheong, H. Liu, H. Song, and J. Tang, ACS Energy Lett. **2**, 2125 (2017).

[9] X. Wen, Y. He, C. Chen, X. Liu, L. wang, B. Yang, M. Leng, H. Song, K. Zeng, D. Li, K. Li, L. Gao, and J. Tang, Sol. Energy Mater. Sol. Cells **172**, 74 (2017).

[10] A.P. Torane and C.H. Bhosale, J. Phys. Chem. Solids **63**, 1849 (2002).

[11] X. Liu, J. Chen, M. Luo, M. Leng, Z. Xia, Y. Zhou, S. Qin, D.-J. Xue, L. Lv, H. Huang, D. Niu, and J. Tang, ACS Appl. Mater. Interfaces **6**, 10687 (2014).

[12] M. Dimitrievska, G. Gurieva, H. Xie, A. Carrete, A. Cabot, E. Saucedo, A. Pérez-Rodríguez, S. Schorr, and V. Izquierdo-Roca, J. Alloys Compd. **628**, 464 (2015).

[13] C. Insignares-Cuello, F. Oliva, M. Neuschitzer, X. Fontané, C. Broussillou, T. de Monsabert, E. Saucedo, C.M. Ruiz, A. Pérez-Rodríguez, and V. Izquierdo-Roca, Sol. Energy Mater. Sol. Cells **143**, 212 (2015).

[14] P. Salomé, P. Fernandes, J. Leitão, M. Sousa, J.P. Teixeira, and A.F. da Cunha, J. Mater. Sci. **49**, 7425 (2014).

[15] Y. Zhang, G. Li, B. Zhang, and L. Zhang, Mater. Lett. **58**, 2279 (2004).

[16] Y. Zhou, M. Leng, Z. Xia, J. Zhong, H. Song, X. Liu, B. Yang, J. Zhang, J. Chen, K. Zhou, J. Han, Y. Cheng, and J. Tang, Adv. Energy Mater. **4**, 1301846 (2014).

[17] K. Nagata, K. Ishibashi, and Y. Miyamoto, Jpn. J. Appl. Phys. **20**, 463 (1981).

[18] G. Mestl, P. Ruiz, B. Delmon, and H. Knozinger, J. Phys. Chem. **98**, 11276 (1994).

[19] A. Shongalova, M.R. Correia, J.P. Teixeira, J.P. Leitão, J.C. González, S. Ranjbarrizi, S. Garud, B. Vermang, J.M.V. Cunha, P.M.P. Salomé, and P.A. Fernandes, Submitted to Sol. Energy Mater. Sol. Cells, Elsevier.

[20] Z.G. Ivanova, E. Cernoskova, V.S. Vassilev, and S. V Boycheva, Mater. Lett. **57**, 1025 (2003).

[21] V.S. Minaev, S.P. Timoshenkov, and V. V Kalugin, J. Optoelectron. Adv. Mater. **7**, 1717 (2005).

[22] X. Wang, K. Kunc, I. Loa, U. Schwarz, and K. Syassen, Phys. Rev. B **74**, 134305 (2006).

[23] Y. Zhao, K.T.E. Chua, C.K. Gan, J. Zhang, B. Peng, Z. Peng, and Q. Xiong, Phys. Rev. B **84**, 205330 (2011).

[24] C. Platzer-Björkman, P. Zabierowski, J. Pettersson, T. Törndahl, and M. Edoff, Prog. Photovoltaics Res. Appl. **18**, 249 (2010).

[25] A. SeJin, K. Ki Hyun, Y. Jae Ho, and Y. Kyung Hoon, J. Appl. Phys. **105**, 113533 (2009).

[26] Z. Li, X. Chen, H. Zhu, J. Chen, Y. Guo, C. Zhang, W. Zhang, X. Niu, and Y. Mai, Sol. Energy Mater. Sol. Cells **161**, 190 (2017).

[27] W.H. Weber and R. Merlin, editors , *Raman Scattering in Materials Science* (Springer Berlin Heidelberg, Berlin, Heidelberg, 2000).

[28] D. Bäuerle, *Laser Processing and Chemistry*, 4th ed. (Springer Berlin Heidelberg, Berlin,

Heidelberg, 2011).

[29] P. Sereni, M. Musso, P. Knoll, P. Blaha, K. Schwarz, and G. Schmidt, in *AIP Conf. Proc.* (2010), pp. 1131–1132.

[30] R. Caracas and X. Gonze, Phys. Chem. Miner. **32**, 295 (2005).

[31] J. Wang, Z. Deng, and Y. Li, Mater. Res. Bull. **37**, 495 (2002).

[32] I. Efthimiopoulos, J. Zhang, M. Kucway, C. Park, R.C. Ewing, and Y. Wang, Sci. Rep. **3**, 2665 (2013).

[33] *International Centre for Diffraction Data—Reference Code, 01-072-1184 (Orthorhombic Pbnm Sb$_2$Se$_3$), 01-072-1334 (Cubic Fd-3m Sb$_2$O$_3$), 00-005-0562 (Rhombohedral R-3m Se$_6$).*